Appl. Phys. A (2016)122:827
DOI 10.1007/s00339-016-0325-z

Applied Physics A
Materials Science & Processing

Durability of the tunable adhesive superhydrophobic PTFE surfaces for harsh environment applications

Yao Fang[1] · Jiale Yong[1] · Feng Chen[1] · Jinglan Huo[1] · Qing Yang[2] · Hao Bian[1] · Guangqing Du[1] · Xun Hou[1]

Received: 5 May 2016 / Accepted: 28 July 2016

Abstract Tunable adhesive superhydrophobic materials have attracted increasing research interest due to their applications in microdroplet manipulation, biological detection and microfluidic system. However, most of the artificial materials easily lose superhydrophobicity in harsh environments. The durability of superhydrophobic materials is very important to extend their lifetime in practical applications. In this paper, bioinspired durable superhydrophobicity with tunable adhesion on polytetrafluoroethylene surfaces is realized via a one-step femtosecond laser irradiation. On the laser-induced superhydrophobic surfaces, the sliding angle can be tuned from 1° to 90° (water droplet is pinned on the surface at any titled angles). The tunable water adhesion results from different contact states which change from the lotus state to the transition state and then to the composite state with increasing average distance of irradiation points. Water droplet quick localization and no-loss droplet transportation were achieved through designing surface adhesion. In addition, the resultant surfaces are so stable that they can maintain superhydrophobicity even after storing in harsh environments, without dramatical superhydrophobicity decay for a long time.

1 Introduction

Lotus leaves and red rose petals are well known for the "lotus effect" and "petal effect," respectively [1–4]. The "lotus effect" exhibits superhydrophobicity with extremely low adhesion [1, 2]. A water droplet can easily roll off a lotus leaf with a slight shaking. On the contrary, the "petal effect" refers superhydrophobicity with extremely high adhesion [3]. Water droplets cannot slide down from a rose petal even when the petal is turned upside down. It has been verified that the "lotus effect" and the "petal effect" are caused by different wetting states which are originated from the surface micro-/nano-structures [1–5]. Water droplet only contacts the peak of the microstructures of a lotus leaf (lotus state), while water droplet can partly impregnate the microstructures on a red rose petal (transition state) [1–3].

Surface wettability is mainly governed by the chemical composition of materials and the surface geometrical microstructures [2, 6–10]. Recently, superhydrophobic surfaces with tunable adhesion have attracted much attention due to their important applications in biological detection [11, 12], no-loss microdroplet manipulation [12–14], microfluidic systems [15], and so on. There are two primary methods to prepare tunable adhesive superhydrophobic surfaces: building continuously adjustable microstructures on the intrinsic hydrophobic materials, using low surface energy molecule to modify the rough hydrophilic materials whose surface microstructure can be continuously controlled [15–23]. Up to now, great efforts are devoted to control the adhesion of superhydrophobic surfaces. For example, Zhao

✉ Feng Chen
chenfeng@mail.xjtu.edu.cn

✉ Hao Bian
haobian@mail.xjtu.edu.cn

[1] Department of Electronic Science and Technology, State Key Laboratory for Manufacturing System Engineering and Key Laboratory of Photonics Technology for Information of Shaanxi Province, School of Electronics and Information Engineering, Xi'an Jiaotong University, Xi'an 710049, People's Republic of China

[2] School of Mechanical Engineering, Xi'an Jiaotong University, Xi'an 710049, People's Republic of China

Published online: 17 August 2016

et al. used polydimethylsiloxane (PDMS) to replicate a Si master mold and achieved patterning superhydrophobic PDMS surface with low and high adhesion, respectively, by adjusting the aspect ratios of simple pillars [20]. Li et al. fabricated well-aligned porous Au surface using electrodeposition and corrosion. After the modification of *n*-hexadecanethiol, switchable adhesion was obtained on the porous Au surface [21]. Zhong et al. built periodic microstructures with different topographies on copper surface via femtosecond laser ablation. After surface chemical modification, the laser-created surface showed superhydrophobicity with tunable adhesion to water [22]. Sun et al. realized reversibly tunable adhesion in situ on a PDMS pillar array film by adjusting the surface curvature [23]. Although the superhydrophobic surfaces with tunable adhesion have been achieved on various materials, those materials may partially lose their superior wettability once they suffer from harsh environments like strong acid or alkali corrosion, high temperature, strong friction. The application range of the artificial superhydrophobic materials is very limited because most practical application environments are generally not mild. The realization of durable superhydrophobic surfaces with tunable adhesion has remained challenging.

Polytetrafluoroethylene (PTFE) is a durable polymer material and has many excellent properties, including anti-acid/alkali, low- and high-temperature resistant (−180–+250 °C), insoluble in organic solvents, strong electrical insulation and aging resistance [24, 25]. Therefore, PTFE material has been widely applied in various fields. In addition, PTFE has a really low surface energy, thereby showing intrinsic hydrophobicity. Thus, we can design micro-/nano-structures on its surface to obtain stable superhydrophobicity. The excellent stability is the advantage of PTFE material, but this property also arises difficulty in building rough micro-/nano-structures on PTFE surfaces when we want to achieve superhydrophobicity by many common methods, such as chemical etching [26], self-assembly [27], rapid thermal annealing [28]. Femtosecond laser has been proved to be an effective tool to achieve controllable microstructures [29–32]. It can be used for structuring a wide range of materials due to its predominant characteristics: ultra-short pulse, ultra-high instantaneous power and precision machining ability [32–34]. Recently, some research groups made a preliminary attempt to prepare superhydrophobic PTFE surfaces by a femtosecond laser. Adhi et al. [24] proved that femtosecond laser irradiation was a chemically clean processing for PTFE. The irradiated PTFE surface remains the same stability as the intrinsic PTFE. Liang et al. [35] fabricated superhydrophobic PTFE surface with a forest of entangled fibers. The as-prepared surface exhibited ultra-low adhesion. Toosi et al. [36] realized a contact angle (CA) of 170° and CA hysteresis of 3° on PTFE surface by biaxial scanning of femtosecond laser. However, the above-mentioned superhydrophobic PTFE surfaces only show ultra-low adhesion. As far as we know, durable superhydrophobic PTFE surfaces with tunable adhesion have not been reported until now.

In this paper, stable superhydrophobicity was achieved on the PTFE surfaces by femtosecond laser ablation. The adhesion of the laser-created superhydrophobic surfaces can be tuned from ultra-low to ultra-high. The relationship between the wettability of the PTFE surface and the process parameter was systematically studied. Ultra-low-adhesive superhydrophobic PTFE surfaces show excellent self-cleaning ability like the lotus leaf, while the ultra-high adhesion superhydrophobic PTFE surface like rose petal can be used as a "mechanical hand" to transport water droplet without any volume loss. Through the specific design of the surface adhesion, water droplet quick localization was realized. Importantly, the obtained superhydrophobicity is very stable even after storing the samples in some harsh environments, endowing the as-prepared superhydrophobic surfaces with a long service life in practical applications.

2 Experimental section

The industrial PTFE (Ligong, China) sheet with the thickness of 1 mm was used in the experiment. The hierarchical microstructure was fabricated on the PTFE surface by a rapid line-by-line femtosecond laser scanning process. The schematic of the processing system is shown in our previous work [15, 31, 32]. The femtosecond laser (pulse duration = 50 fs; central wavelength = 800 nm; frequency = 1 kHz) is produced by a regenerative amplified Ti: sapphire laser system (Coherent Libra-usp-he). The laser beam was focused on the PTFE surface by an objective lens (20, NA = 0.4, Nikon). After irradiation, the samples were cleaned by acetone, alcohol and deionized water. The laser power was changed by a rotating attenuator. The average distance (AD) of irradiation points was adjusted by changing the scanning speed and scanning interval.

The morphology of the laser-ablated surfaces was observed by a Quanta FEG 250 scanning electron microscope (SEM, FEI, America). The CA and sliding angle (SA) of a 7-μL deionized water droplet on the samples were measured by a JC2000D contact-angle system (Powereach, China). The average value was obtained by measuring five different positions of each sample. The snapshots of the water droplet bounce process were taken by a high-speed CCD with 100 frames per second. For the self-cleaning test, PTFE surface was deliberately polluted by some blue chalk powder.

3 Results and discussion

Figure 1 shows the typical SEM images of the as-prepared PTFE samples with different ADs at the laser power of 30 mW. As shown in Fig. 1a, e, the laser-irradiated area is covered by microscale protrusions randomly decorating with some nano-structures which are like stone flowers in a Karst cave. With increasing AD, the size of microscale structures constantly increases (Fig. 1a–c, e–g). When the AD increases above 11 μm, the laser-ablated craters separate from each other and produce a heterogeneous pattern (Fig. 1d, h). At present, some intrinsic PTFE areas appear. The diameter of the craters is about 11 ± 2 μm. The ratio of the intrinsic non-irradiated area to the laser-induced area increases with enlarging the AD.

The inset of each image in Fig. 1 shows the behavior of a water droplet on the corresponding sample, including both static (Fig. 1a–d) and dynamic (Fig. 1e–h) states. The relationship between the surface wettability and the AD is shown in Fig. 2. Obviously, these curves for the samples irradiated at different laser power (30, 20, 10 mW) are similar to each other. With increasing AD, the CA decreases slightly, while the SA, as well as the adhesion, shows a drastic change.

In the case of 30 mW, the as-prepared surfaces show superhydrophobicity when AD is less than 11 μm. The insets of Fig. 1a, b show the droplet shapes with CAs of 153° (AD = 4 μm) and 152.5° (AD = 10 μm), respectively. When AD is equal to 11 μm, CA is almost 150° which is the standard of superhydrophobicity [37, 38]. The tendency of the SA curve shows a distinct difference from CA's. When AD is no more than 8 μm, SAs are all less than 10°, indicating extremely low adhesion. The adhesion of the rough PTFE surface can be drastically tuned from ultra-low to ultra-high when AD value increases from 8 to 11 μm. For the samples with AD ≥ 11 μm, the water droplet will adhere to the PTFE surface and will not roll off even when the sample is turned upside down. Likewise,

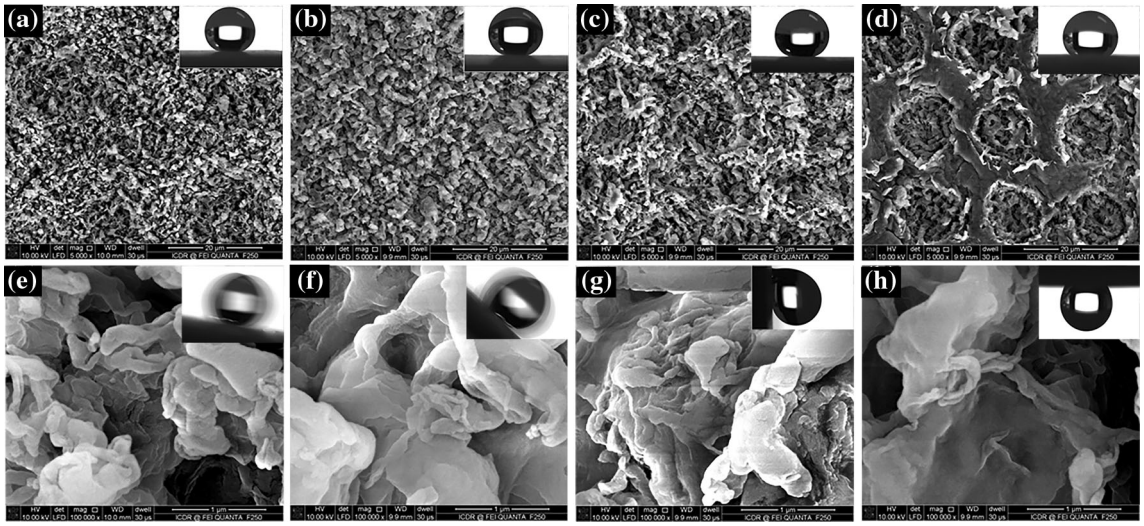

Fig. 1 Low- and high-magnification SEM images of the laser-ablated PTFE surfaces with different ADs at a laser power of 30 mW: **a**, **e** AD = 4 μm; **b**, **f** AD = 10 μm; **c**, **g** AD = 11 μm; **d**, **h** AD = 18 μm. The *insets* of **a**–**d** show the static states of a 7-μL water droplet on the samples, while the *insets* of **e**–**h** show the dynamic property

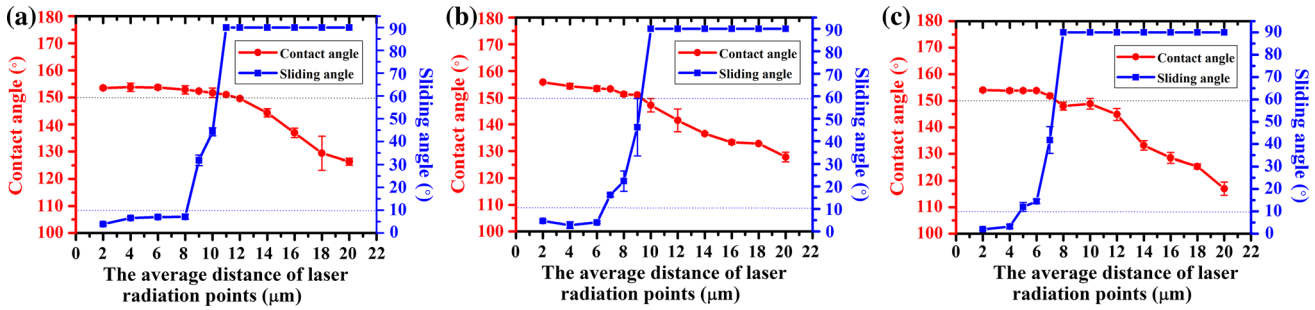

Fig. 2 Dependence curve between the average distance of laser radiation points and the CA (*left*)/SA (*right*): **a** laser power = 30 mW; **b** laser power = 20 mW; **c** laser power = 10 mW

superhydrophobic surfaces with tunable adhesion can also be achieved at the laser power of 20 mW (Fig. 2b) and 10 mW (Fig. 2c).

Water droplet bouncing behavior is also usually used to characterize the surface adhesion besides SA [39–41]. In Fig. 3, a 14-μL water droplet was released from a height of 2.3 mm above the as-prepared PTFE surfaces. The water droplet speeded up during the free-falling motion. After the droplet contacted the as-prepared surface, the kinetic energy gradually transformed into elastic potential energy with the increased elastic deformation. Then, an inverse process happened. The elastic potential energy was returned to kinetic energy, while the adhesion of the surface would prevent this motion. The magnitude of the surface adhesion determined whether the water can bounce off the surface and how many times can it bounce. The water droplet can rebound for 5 times after impacting the surface (AD of 4 μm) with ultra-low adhesion (Fig. 3a). The amount of rebound times decreases with increasing AD. For the sample with AD = 10 μm, the water droplet can only rebound for 1 time (Fig. 3b). Ultimately, the droplet can not rebound when AD increases to 14 μm (Fig. 3c) because of the ultra-high adhesion. The bouncing behaviors further verify the tunable adhesion of the femtosecond laser-irradiated PTFE surfaces.

In 2003, Railkar et al. demonstrated that the femtosecond laser irradiation of PTFE is a chemically clean processing [24]. The chemical composition of PTFE surface does not change during femtosecond laser ablation. The wettability of solid materials is mainly governed by their chemical composition and surface geometrical microstructure, so the tunable adhesion of the laser-induced PTFE surfaces is primarily resulted from the variation of surface microstructures which can induce different liquid–solid contact states. For the PTFE surfaces (30 mW, AD $\leq$ 8 μm) whose microstructure is more abundant and the size is smaller, the water droplet only contacts the peak of the micro-/nano-hierarchical structures, as shown in Fig. 4a. An air layer exists between the droplet and the PTFE substrate. The contact area between the droplet and the laser-induced rough microstructure is so small that the sample only provides extremely low adhesion for the water droplet; therefore, the droplet can easily roll down the surface. This contact state is usually called lotus state. With increasing the size of the microstructures, the contact state will turn to the transition state (Fig. 4b) which induces a modest adhesion. Water droplet can partly penetrate the valley of the fabricated microstructures. With increasing AD, more water is trapped in the rough microstructures, resulting in a bigger solid–water contact area and a thinner trapped air cushion. The SA and water adhesion also increase. When the microstructures are big enough, a water droplet can contact rough PTFE surface sufficiently. Extremely high adhesion generates between the surface and the water droplet. The water droplet can be firmly pinned on the sample surface even when the sample is turned upside down. Furthermore, for an even larger AD value, there are some non-irradiated areas on the PTFE

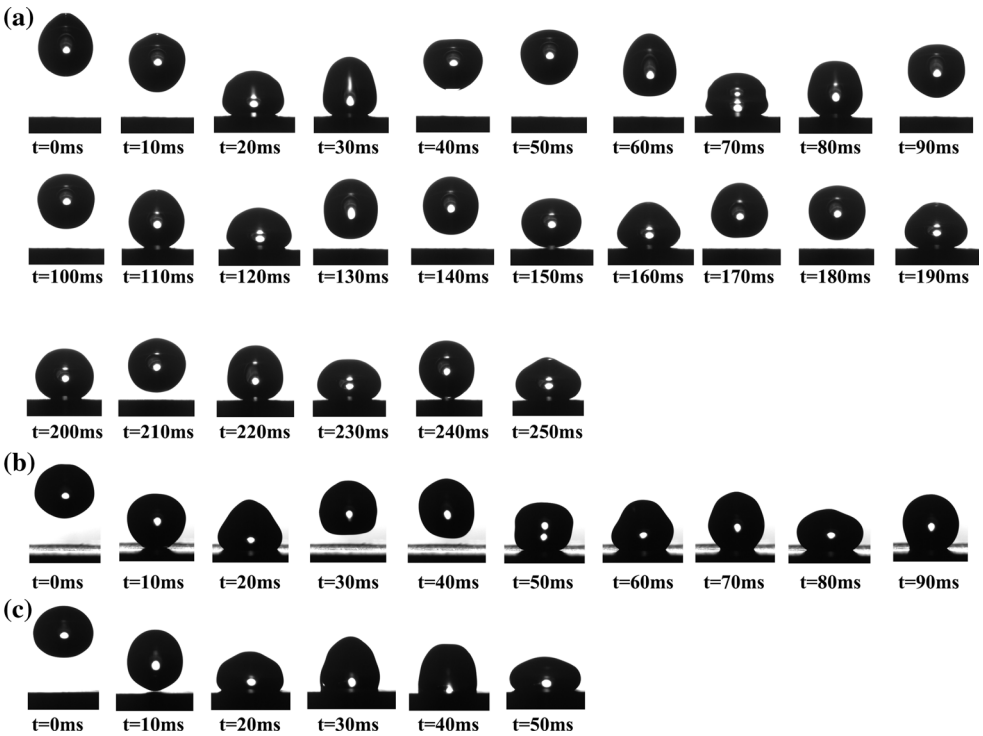

Fig. 3 Snapshots of a 14-μL water droplet impact on the as-prepared PTFE surfaces with different ADs: **a** 4 μm, **b** 10 μm, **c** 14 μm. All the samples were fabricated at the laser power of 30 mW

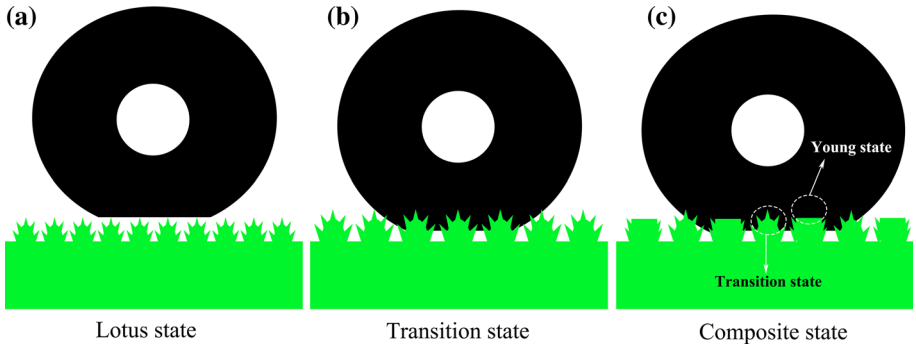

Fig. 4 Schematic illustration of different solid–liquid contact states: **a** lotus state, **b** transition state, **c** composite state

surface, as shown in Fig. 1d. A water droplet contacts not only the rough areas (transition state) but also the intrinsic PTFE surface (Young state). This contact state can be considered as a composite state (Fig. 4c), giving rise to a smaller CA, but an extra-large SA remained 90°. So at the transition state, we can tune the adhesion of the PTFE surface by adjusting AD.

To verify the contact states further, we fabricated three neighboring laser-irradiated regions with different ADs (4, 7, 12 μm), at the laser power of 10 mW. As shown in Fig. 2c, these three parts correspond to lotus state, transition state and composite state, respectively. Figure 5a shows three methylene blue-dyed water droplets on the as-prepared area with different AD values. All the droplets keep sphere shape, exhibiting superhydrophobicity. When the sample was immersed in water, three silver mirror-like interfaces appeared on the laser-ablated domains (Fig. 5b). These "mirrors" result from total reflection of light [42]. The brightness of the "mirrors" slowly diminishes with increasing AD from 4 to 12 μm, indicating that the area of water and the trapped air layer interface becomes smaller (Fig. 4). The trend of this change agrees well with that the contact state shifts from lotus state to transition state and even to composite state.

The ultra-low-adhesive superhydrophobic PTFE surface (30 mW, AD = 4 μm) exhibits excellent self-cleaning ability, which is a significant characteristic of lotus effect [8]. As shown in Fig. 6a, the surface was deliberately polluted by some blue chalk powder first. As a result, the blue powder became scattered around the surface. Then, a water droplet was carefully put on the polluted surface which was slightly titled. The water droplet rolled down, leaving a clean track. In the process of rolling off, the water droplet collected the pollution on the track and became muddy. The self-cleaning ability makes the as-prepared PTFE surfaces possess ultra-low adhesion even in the vulnerable polluted environment, showing a great advantage in practical applications.

In general, durability plays a very important role for the superhydrophobic materials to long-term practical applications. The ultra-low-adhesive superhydrophobicity of the as-prepared PTFE surface is very stable. The laser-induced rough PTFE surface (30 mW, AD = 4 μm) can keep its original superhydrophobicity and ultra-low adhesion even

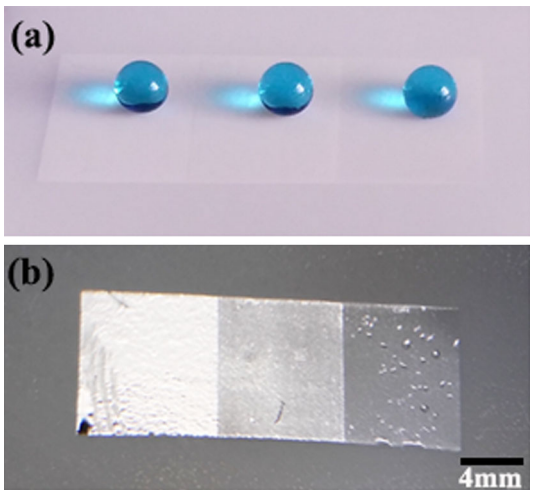

Fig. 5 Photographs of a PTFE surface consisting of three neighboring laser-irradiated regions with different ADs, *left* to *right*—4, 7, 12 μm, at laser power of 10 mW. **a** Three water droplets on each fabricated area. **b** The sample shows different silver mirror-like reflectance in water

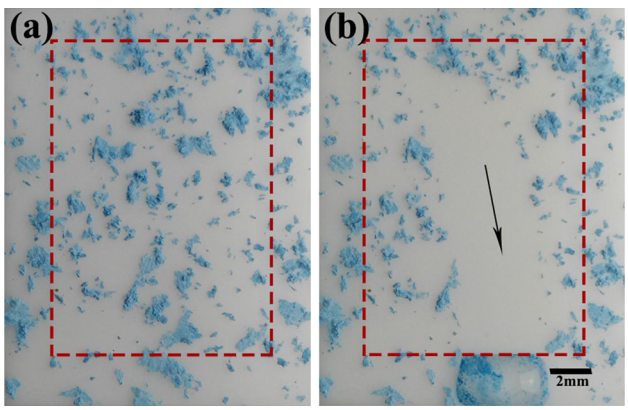

Fig. 6 Self-cleaning test of the as-prepared superhydrophobic PTFE surface with ultra-low adhesion. **a** polluting the sample with some blue chalk powder, **b** a water droplet rolling away

after storing in a series of harsh environments for 1 day: high temperature (250 °C), 40 % hydrofluoric acid solution, 98 % concentrated sulfuric acid, aqua regia and 10 M sodium hydroxide solution, as showing in Fig. 7. In addition, the as-prepared surface maintains almost the same superhydrophobicity for the water droplet with different pH values. The stability of superhydrophobicity makes the laser-ablated rough PTFE surface be applied more widely than other ordinary superhydrophobic surfaces.

Droplet quick localization is significant in controlling liquid movement. It can be realized via designing adhesion in different areas according to the requirement. As shown in Fig. 8, two neighboring areas with different adhesion were fabricated in a PTFE substrate. The left and right regions of the laser-ablated part were fabricated at the AD of 4 and 7 μm, respectively. The laser power used was 10 mW. The left part performs ultra-low adhesion, while the right part shows ultra-high adhesion (Fig. 2c). If a water droplet was released on the lower-adhesive areas with the sample being tilted a small angle, the droplet would roll off the left region. However, it would be pinned on the sample as soon as the droplet contacted the right region. The kinetic energy of the water droplet transformed into internal energy and elastic potential energy. The elastic potential energy would further transform into internal energy during the process of water droplet damped swing motion (Fig. 8e–g). Finally, the water droplet stopped and rested on the specific area. As a result, the water droplet was quickly positioned on the pre-designed region with higher adhesion.

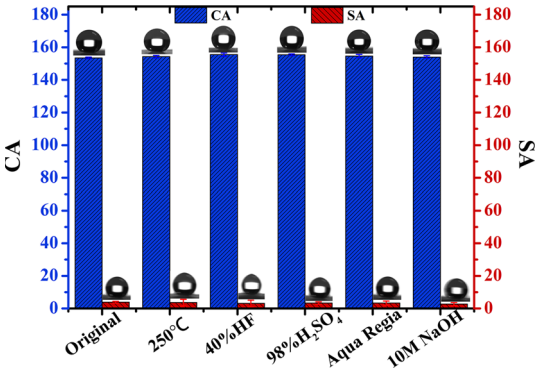

Fig. 7 CAs and SAs of 7-μL water droplets on the as-prepared surface after storing in different harsh environments for 1 day (30 mW, AD = 4 μm)

The superhydrophobic PTFE surface with ultra-high adhesion can be used to transfer water droplet without any volume loss, as shown in Fig. 9. A 7-μL water droplet was firstly put on a low-adhesive superhydrophobic PTFE surface (30 mW, AD = 4 μm). Then, the "mechanical hand" with ultra-high adhesion (30 mW, AD = 12 μm) was lowered down to contact the water droplet (Fig. 9a, b). As a result, the water droplet was adhered on the "mechanical hand" surface. When the "mechanical hand" was lifted up, the water droplet would detach from the ultra-low-adhesive substrate and shift to the "mechanical hand" because of higher adhesive force, as shown in Fig. 9c. After shifting the droplet to the place right above the destination, the water droplet was lowered down, contacted and released on the target PTFE surface (30 mW, AD = 14 μm) with a higher adhesion than the "mechanical hand" (Fig. 8d, e). Importantly, there was no obvious volume loss of water droplet throughout the whole process. This special ability

Fig. 8 Process of water droplet quick localization

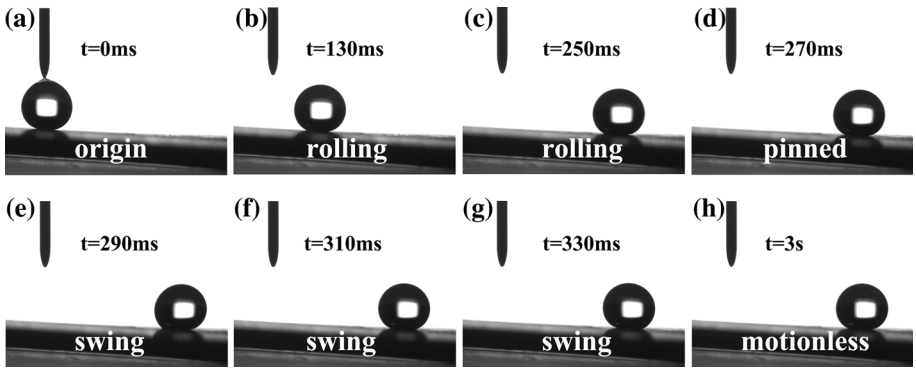

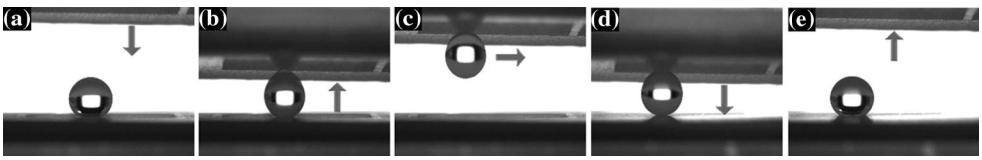

Fig. 9 Process of no-loss droplet transportation. The "mechanical hand" is a high-adhesive superhydrophobic PTFE surface (30 mW, AD = 12 μm)

endows the superhydrophobic PTFE surface with more applications such as biomedical testing, chemical micro-liquid research.

4 Conclusions

In conclusion, stable superhydrophobicity was achieved on the PTFE surfaces by femtosecond laser ablation. The adhesion of the laser-created superhydrophobic surfaces can be tuned from ultra-low to ultra-high. On the laser-induced superhydrophobic surfaces, the CA of a water droplet is above 150°, while the SA can be tuned from 1° to 90° with increasing AD. The tunable water adhesion results from different contact states which change from the lotus state to the transition state and then to the composite state. Superhydrophobic PTFE surface with ultra-low adhesion, like lotus leaves, shows excellent bounce property and self-cleaning ability. With tunable adhesion, water droplet quick localization and transportation were achieved. More importantly, the as-prepared surfaces are so stable that they keep their superior wettability even after storing in a harsh environment for a long time. The durable superhydrophobic PTFE surfaces with tunable adhesion can be used in self-cleaning, microdroplet manipulation, biological detection and microfluidic system regardless of harsh environments.

Acknowledgments This work was supported by the National Science Foundation of China under the Grant Nos. 61275008, 51335008 and 61475124, the Special-Funded Program on National Key Scientific Instruments and Equipment Development of China under the Grant No. 2012YQ12004706, the Collaborative Innovation Center of Suzhou Nano Science and Technology and the International Joint Research Center for Micro/Nano Manufacturing and Measurement Technologies. The SEM work was done at International Center for Dielectric Research (ICDR), Xi'an Jiaotong University; we really appreciate Dai Yanzhu's help for obtaining SEM images.

References

1. A. Marmur, Langmuir **20**, 3517–3519 (2011)
2. V. Zorba, E. Stratakis, M. Barberoglou, E. Spanakis, P. Tzanetakis, S.H. Anastasiadis, C. Fotakis, Adv. Mater. **20**, 4049–4054 (2008)
3. L. Feng, Y. Zhang, J. Xi, Y. Zhu, N. Wang, F. Xia, L. Jiang, Langmuir **24**, 4114–4119 (2008)
4. X. Zhang, F. Shi, J. Niu, Y. Jiang, Z. Wang, J. Mater. Chem. **18**, 621–633 (2008)
5. W. Barthlott, C. Neinhuis, Planta **202**, 1–8 (1997)
6. T. Sun, G. Qing, Adv. Mater. **23**, H57–H77 (2011)
7. K. Liu, L. Jiang, Nano Today **6**, 155–175 (2011)
8. J. Genzer, K. Efimenko, Biofouling **22**, 339–360 (2006)
9. F. Shi, J. Niu, J. Liu, F. Liu, Z. Wang, X. Feng, X. Zhang, Adv. Mater. **19**, 2257–2261 (2007)
10. G. Ju, M. Cheng, M. Xiao, J. Xu, K. Pan, X. Wang, Y. Zhang, F. Shi, Adv. Mater. **25**, 2915–2919 (2013)
11. W. Song, D.D. Veiga, C.A. Custódio, J.F. Mano, Adv. Mater. **21**, 1830–1834 (2009)
12. X. Hong, X. Gao, L. Jiang, J. Am. Chem. Soc. **129**, 1478–1479 (2007)
13. N. Zhao, Q. Xie, X. Kuang, S. Wang, Y. Li, X. Lu, S. Tan, J. Shen, X. Zhang, Y. Zhang, J. Xu, C.C. Han, Adv. Funct. Mater. **17**, 2739–2745 (2007)
14. M.H. Jin, X.J. Feng, L. Feng, T.L. Sun, J. Zhai, T.J. Li, L. Jiang, Adv. Mater. **17**, 1977–1981 (2005)
15. D. Zhang, F. Chen, Q. Yang, J. Yong, H. Bian, Y. Ou, J. Si, X. Meng, X. Hou, A.C.S. Appl, Mater. Interfaces **4**, 4905–4912 (2012)
16. Z. Hu, X. Zhang, Z. Liu, K. Huo, P.K. Chu, J. Zhai, L. Jiang, Adv. Funct. Mater. **24**, 6381–6388 (2014)
17. M.K. Dawood, H. Zheng, T.H. Liew, K.C. Leong, Y.L. Foo, R. Rajagopalan, S.A. Khan, W.K. Choi, Langmuir **27**, 4126–4133 (2011)
18. L. Heng, X. Meng, B. Wang, L. Jiang, Langmuir **29**, 9491–9498 (2013)
19. B. Bhushan, Langmuir **28**, 1698–1714 (2012)
20. H. Shahsavan, D. Arunbabu, B. Zhao, Macromol. Mater. Eng. **297**, 743–760 (2012)
21. X. Mo, Y. Wu, J. Zhang, T. Hang, M. Li, Langmuir **31**, 10850–10858 (2015)
22. J. Long, P. Fan, D. Gong, D. Jiang, H. Zhang, L. Li, M. Zhong, A.C.S. Appl, Mater. Interfaces **7**, 9858–9865 (2015)
23. D. Wu, S. Wu, Q. Chen, Y. Zhang, J. Yao, X. Yao, L. Niu, J. Wang, L. Jiang, H. Sun, Adv. Mater. **23**, 545–549 (2011)
24. K.P. Adhi, R.L. Owings, T.A. Railkar, W.D. Brown, A.P. Malshe, Appl. Surf. Sci. **218**, 17–23 (2003)
25. S.K. Biswas, K. Vijayan, Wear **158**, 193–211 (1992)
26. J. Li, X. Liu, Y. Ye, H. Zhou, J. Chen, J. Phys. Chem. C **115**, 4726–4729 (2011)
27. Y. Li, E.J. Lee, S.O. Cho, J. Phys. Chem. C **111**, 14813–14817 (2007)
28. S.S. Chhatre, A. Tuteja, W. Choi, A. Revaux, D. Smith, J.M. Mabry, G.H. McKinley, R.E. Cohen, Langmuir **25**, 13625–13632 (2009)
29. J. Yong, F. Chen, Q. Yang, X. Hou, Soft Matter **11**, 8897–8906 (2015)
30. Z. Deng, F. Chen, Q. Yang, H. Bian, G. Du, J. Yong, C. Shan, X. Hou, Adv. Funct. Mater. **26**, 1995–2001 (2016)
31. J. Yong, F. Chen, Q. Yang, U. Farooq, X. Hou, J. Mater. Chem. A **3**, 10703–10709 (2015)
32. J. Yong, F. Chen, Q. Yang, G. Du, C. Shan, H. Bian, U. Farooq, X. Hou, J. Mater. Chem. A **3**, 9379–9384 (2015)
33. J. Yong, F. Chen, Q. Yang, Y. Fang, J. Huo, X. Hou, Chem. Commun. **51**, 9813–9816 (2015)
34. A.Y. Vorobyev, C. Guo, Appl. Phys. Lett. **92**, 041914 (2008)
35. F. Liang, J. Lehr, L. Danielczak, R. Leask, A. Kietzig, Int. J. Mol. Sci. **15**, 13681–13696 (2014)
36. S.F. Toosi, S. Moradi, S. Kamal, S.G. Hatzikiriakos, Appl. Surf. Sci. **349**, 715–723 (2015)
37. Z. Chu, S. Seeger, Chem. Soc. Rev. **43**, 2784–2798 (2014)
38. L. Wen, Y. Tian, L. Jiang, Angew. Chem. Int. Edit. **54**, 3387–3399 (2015)
39. Y.C. Jung, B. Bhushan, Langmuir **24**, 6262–6269 (2008)
40. Q.B. Zhang, D. Xu, T.F. Hung, K. Zhang, Nanotechnology **24**, 065602 (2013)
41. Y.C. Jung, B. Bhushan, Langmuir **25**, 9208–9218 (2009)
42. I.A. Larmour, S.E.J. Bell, G.C. Saunders, Angew. Chem. **119**, 1740–1742 (2007)